# Interaction of Acetate Anion with Hydrated $Al^{3+}$ Cation: A Theoretical Study

**Daniel Tunega,*,†,‡ Georg Haberhauer,‡ Martin Gerzabek,‡ and Hans Lischka†**

*Institute for Theoretical Chemistry and Structural Biology, University of Vienna, Währingerstrasse 17, A-1090 Vienna, Austria, and Austrian Research Centers Seibersdorf, A-2444 Seibersdorf, Austria*

*Received: February 22, 2000; In Final Form: May 3, 2000*

Density-functional theory (DFT) methods were used for investigations on the aluminum−hexaaquo complex and on aqueous aluminum−acetate complexes. Solvent effects were computed by means of the polarized continuum model (PCM). Extensive basis set studies and comparison of several functionals lead to efficient and accurate procedures which were applied to the computation of aluminum−acetate complexes. A variety of structural arrangements such as monodentate or bidentate with respect to the bonding of the carboxylate group or cis/trans with respect to the relative position of two acetate molecules were considered. $\Delta H$ and $\Delta G$ values were calculated for the substitution reaction of water molecules in the aluminum−hexaaquo complex by acetate anions. Characteristic differences in $\Delta S$ were found depending on the number of water molecules released per acetate. Overall, we find that monodentate structures are only slightly preferred over bidentate ones and that we expect a relatively complicated system of chemical equilibria without any dominant complex.

## I. Introduction

The aluminum cation plays an important role in soil chemistry. Free forms of Al cations (e.g., the hexaaquo complex) can readily penetrate into plant organisms and can cause aluminum toxicity for plants.[1−3] Soluble aluminum and some other metal cations (such as $Zn^{2+}$, $Fe^{2+}$, $Fe^{3+}$, or $Cd^{2+}$) in high concentration affect the quality of natural sources of water negatively. Larger quantities of $Al^{3+}$ can be released into soil water by dissolution processes of clay minerals.[4−6] Organic acids affect chemical soil processes strongly and speed up the process of dissolution of aluminosilicate minerals considerably. They also influence the weathering and diagenesis of minerals.[4] The formation of stable complexes of organic acids with free Al cations has also important consequences on plant growth and nutrition since aluminum is stabilized as complex and is less phytotoxic.

Chemical processes in soils have been studied extensively. One particular important process is the aforementioned formation of complexes with organic acids such as acetic acid. In order to obtain quantitative information on the stabilities of these complexes, solubility measurements on minerals such as bayerite, boehmite, and gibbsite as well as potentiometric investigations have been carried out.[5−9] The quantitative analysis of these measurements and the evaluation of equilibrium constants and speciation data require the analysis of complex thermodynamic models consisting of many coupled dissociation and association equilibria. These models give a good global picture of the thermodynamic stability of the various constituents. However, they do not give information on detailed structural possibilities and on their relative stabilities.

Quantum-chemical approaches have been used in several studies to determine binding energies and hydration energies of di- and trivalent cations.[10−17] Various structural models of aqueous aluminum−acetate complexes have been investigated using SCF and MP2 calculations.[18−20] One major issue for the accurate calculation of such complexes in solution is the consideration of solvation effects. Since several of the molecular species like the aluminum−hexaaquo complex or deprotonated organic acids (like the acetate anion) carry net charges, solvation energies will be very large. Moreover, since in chemical reactions such as

$$[Al(H2O)_6]^{3+} + Ac^- \rightarrow [Al(H2O)_5Ac]^{2+} + H_2O \quad (1)$$

at least partial charge compensation occurs, the effect of solvation on reaction energies can be even more significant.

Aluminum−acetate complexes were studied thoroughly by Kubicki et al.[18] as isolated species using SCF and MP2 methods and medium-sized basis sets. In a subsequent work, solvation effects were included by Kubicki et al.[20] using a continuum model. The inclusion of solvation contributions improved the agreement of calculated and experimental results (e.g., for reaction 1) considerably. However, there remained still significant discrepancies due to the limitations in the quantum chemical procedures used.

The aim of the present work was twofold. In the first part, we investigated the individual factors affecting the accuracy of the quantum chemical calculation of aluminum complexes. Our strategy was to select an appropriate functional for the DFT method by comparison with ab initio methods containing electron correlation (MP2 method) and to construct efficient and compact basis sets. We choose a polarized continuum model based on a self-consistent reaction field[21−23] for the calculation of solvent effects, similar to the one by Kubicki et al.[20] The aluminum−hexaaquo complex served as a benchmark example.

In the second part of our investigations we applied our techniques to the calculation of the structure and stability of several aluminum−acetate complexes ranging from one to three acetate molecules. A variety of structural arrangements such as monodentate or bidentate with respect to the bonding of the carboxylate group or cis/trans with respect to the relative position of two acetate molecules exist. Possible intramolecular proton transfer or hydrogen bonding can complicate the situation even more. The potentiometric and solubility measurements mentioned already above[5−9] do not provide any of this structural

* To whom correspondence should be addressed: daniel.tunega@univie.ac.at. Permanent address: Institute of Inorganic Chemistry, Slovak Academy of Sciences, Dúbravská cesta 9, SK-84236 Bratislava, Slovakia.

† University of Vienna.

‡ Austrian Research Centers Seibersdorf.

10.1021/jp000699v CCC: $19.00 
Published on Web 07/01/2000

**TABLE 1: Basis Sets[28,29]**

| basis set | aluminum[a] | oxygen[a] | hydrogen[a] |
|---|---|---|---|
| SVP | (10s7p1d)/[4s3p1d] | (7s4p1d)/[3s2p1d] | (3s1p)/[2s1p] |
| SVP+sp[b] | (10s7p1d)/[4s3p1d] | (8s5p1d)/[4s3p1d] | (3s1p)/[2s1p] |
| SVP+spd[c] | (10s7p1d)/[4s3p1d] | (8s5p2d)/[4s3p2d] | (3s1p)/[2s1p] |
| DZP | (11s7p1d)/[6s4p1d] | (8s4p1d)/[4s2p1d] | (4s1p)/[2s1p] |
| TZP | (12s9p1d)/[7s5p1d] | (10s6p1d)/[6s3p1d] | (5s1p)/[3s1p] |
| TZVP | (14s9p1d)/[5s4p1d] | (11s6p1d)/[5s3p1d] | (5s1p)/[3s1p] |
| TZVPP | (14s9p2d1f)/[5s5p2d1f] | (11s6p2d1f)/[5s3p2d1f] | (5s2p1d)/[3s2p1d] |
| QZP(O)[d] | (14s9p2d1f)/[5s5p2d1f] | (11s6p3d1f)/[6s4p2d1f] | (5s2p1d)/[3s2p1d] |

[a] Primitive basis in parentheses, contraction in brackets. [b] One diffuse set of s and p functions on oxygen. [c] One diffuse set of s, p, and d functions on oxygen. [d] QZP basis set on the oxygen atom.

information. Moreover, reactions such as the one given in eq 1 cannot be observed directly since they are embedded in a large set of coupled reactions and equilibria under the given experimental conditions. The aluminum−hexaaquo complex represents the basic reactant for the formation of acetate complexes. $Al^{3+}$ has amphoteric character and can also form a broad scale of hydroxo−aquo complexes from four-coordinated $Al^{3+}$ in the $[Al(OH)_4]^-$ anion to six-coordinated $Al^{3+}$ in the $[Al(H2O)_6]^{3+}$ cation. In this work we focused on octahedrally coordinated $Al^{3+}$ structures which are dominating in a pH range <5 and where the formation of acetate complexes occurs.[6] We present in this study the formation, energetics, and structural parameters of various mono- and bidentate aqueous aluminum−acetate complexes and, after including long-range solvent effect into the calculations, we compute properties for the liquid phase. On the basis of these investigations, we are able to predict the thermodynamic stability of the individual aluminum−acetate structures and to give an evaluation which species should actually exist under the given thermodynamic conditions.

## II. Computational Details

Most of the calculations were performed at the DFT level of the theory. For comparison, SCF and MP2 calculations were carried out as well. The calculations were performed using the Turbomole[24,25] and Gaussian98[26] packages, respectively. Since there is a quite large variety of functionals in DFT available, our first step was to test some of them and to select an appropriate one on the basis of comparisons with MP2 calculations and previous results in the literature. We tested the following standard functionals: SVWN, BVWN, BVWNP, BLYP, B3LYP. For an overview of these methods, see e.g. ref 27.

For our basis set investigations, we used the series of basis sets developed by the group of Ahlrichs[28,29] ranging from SV (split valence) to TZ (triple-ζ) quality. They all include at least one set of polarization functions and are listed in Table 1. Especially, the smaller basis sets are lacking diffuse functions needed for the description of the wave function in the intermolecular region. After some test calculations we decided to augment the SVP basis on oxygen and carbon with a set of diffuse sp and spd functions, respectively. The exponents of these functions were obtained by dividing the smallest respective exponent of the SVP basis by a factor of 3. The abbreviations SVP+sp and SVP+spd are used for these basis sets. As the results below show, these basis sets provide a very efficient way for the description of the interaction of the water and acetate molecules with $Al^{3+}$. We also used a basis set of QZP quality on the oxygen atom. This basis set was constructed from the original TZVPP basis set of oxygen by splitting the first s (6 functions) and p (4 functions) contraction into two contractions containing 3 s and 2 p functions, respectively. This basis set is denominated QZP(O) (see Table 1). The MP2 calculations were carried out with the TZP basis set.

Basis set superposition error (BSSE) corrections[30] to the energy of the formation of the $[Al(H_2O)_6]^{3+}$ complex were calculated for selected basis sets as the difference between the calculated energy of $Al^{3+}$ and the energy of the 6 water molecules in the optimized geometry of the $[Al(H_2O)_6]^{3+}$ complex using the basis set of the $[Al(H_2O)_6]^{3+}$ complex.

All test and benchmark calculations were performed on the aluminum−hexaaquo complex $[Al(H_2O)_6]^{3+}$ in $T_h$ symmetry. $T_h$ is the symmetry of the true minimum which was confirmed by calculation of the eigenvalues of the Hessian at the optimized geometry. This finding is in accordance with calculations of Kubicki et al.[18] and of Wasserman et al.,[15] although in the work of Probst and Hermansson[11] a $D_{2h}$ symmetry structure was obtained.

In the case of the aqueous aluminum−acetate complexes the following structures were studied (see Figure 1): monodentate $[Al(H_2O)_5Ac]^{2+}$, bidentate $[Al(H_2O)_4Ac]^{2+}$, monodentate $[Al(H_2O)_4Ac_2]^+$ (cis and trans), bidentate $[Al(H_2O)_2Ac_2]^+$ (cis and trans), and $AlAc_3$. Since Benezeth et al.[9] found that monodentate hydroxoacetate complex $[Al(H_2O)_4AcOH]^+$ occurs in significant concentrations at higher temperatures and over the pH range 3.2−4.5, we investigated this complex also together with the aqueous hydroxoaluminum $[Al(H_2O)_5OH]^{2+}$ complex. On the basis of energetic similarities between cis and trans forms of the acetate complexes only the cis form of the hydroxoacetate complex was studied. Full geometry optimizations were performed in each case at the BLYP/SVP+sp level which had been selected on the base of test calculations on the $[Al(H_2O)_6]^{3+}$ complex.

Two series of calculations were always carried out: one set for the isolated species (denoted subsequently as "gas phase") and the second one with inclusion of solvation effects based on the self-consistent reaction field (SCRF) method. The latter calculations are denominated as "liquid phase" or in "solution". In the SCRF calculations Tomasi's polarized continuum model (PCM)[21−23] with the cavity defined as series of overlapping spheres and numerical reaction field was used. For the static dielectric constant $\epsilon_0$ of the continuum the value 78.54 of water at 298.15 K was chosen. Also, in the PCM calculations full geometry optimizations of all species were performed at the BLYP/SVP+sp level.

We also performed calculations of vibrational frequencies and of thermochemical data for all complexes. These calculations were carried out on the isolated systems (gas phase) only. In order to describe reactions in solution, calculated solvation energies were added. Since the dielectric constant of a polarizable medium is temperature dependent, we also performed in one case thermochemical calculations at several temperatures and corresponding PCM calculations with different $\epsilon_0$ values. These values were calculated on the base of empirical formula[31]

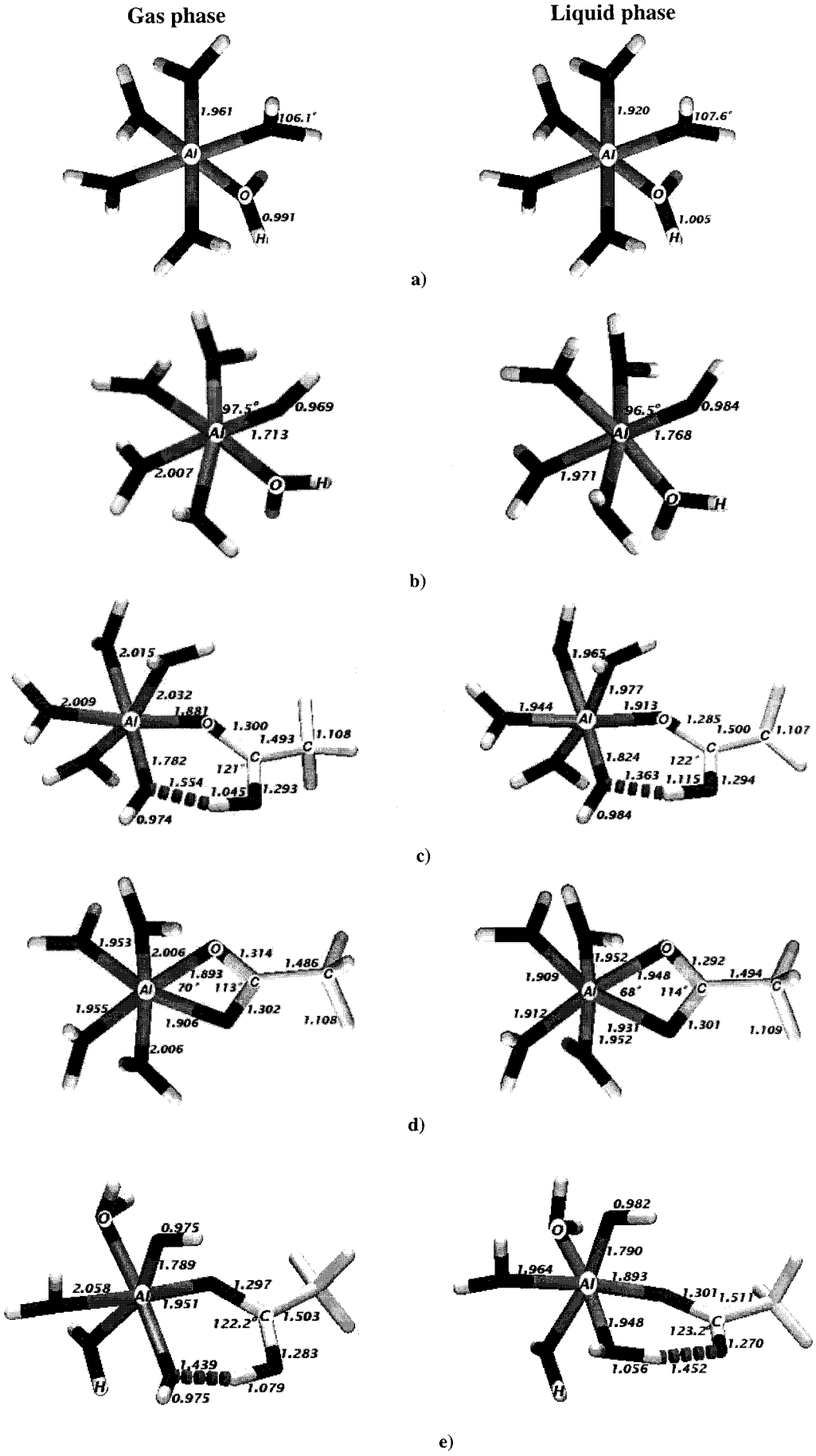
Gas phase
Liquid phase
a)
b)
c)
d)
e)

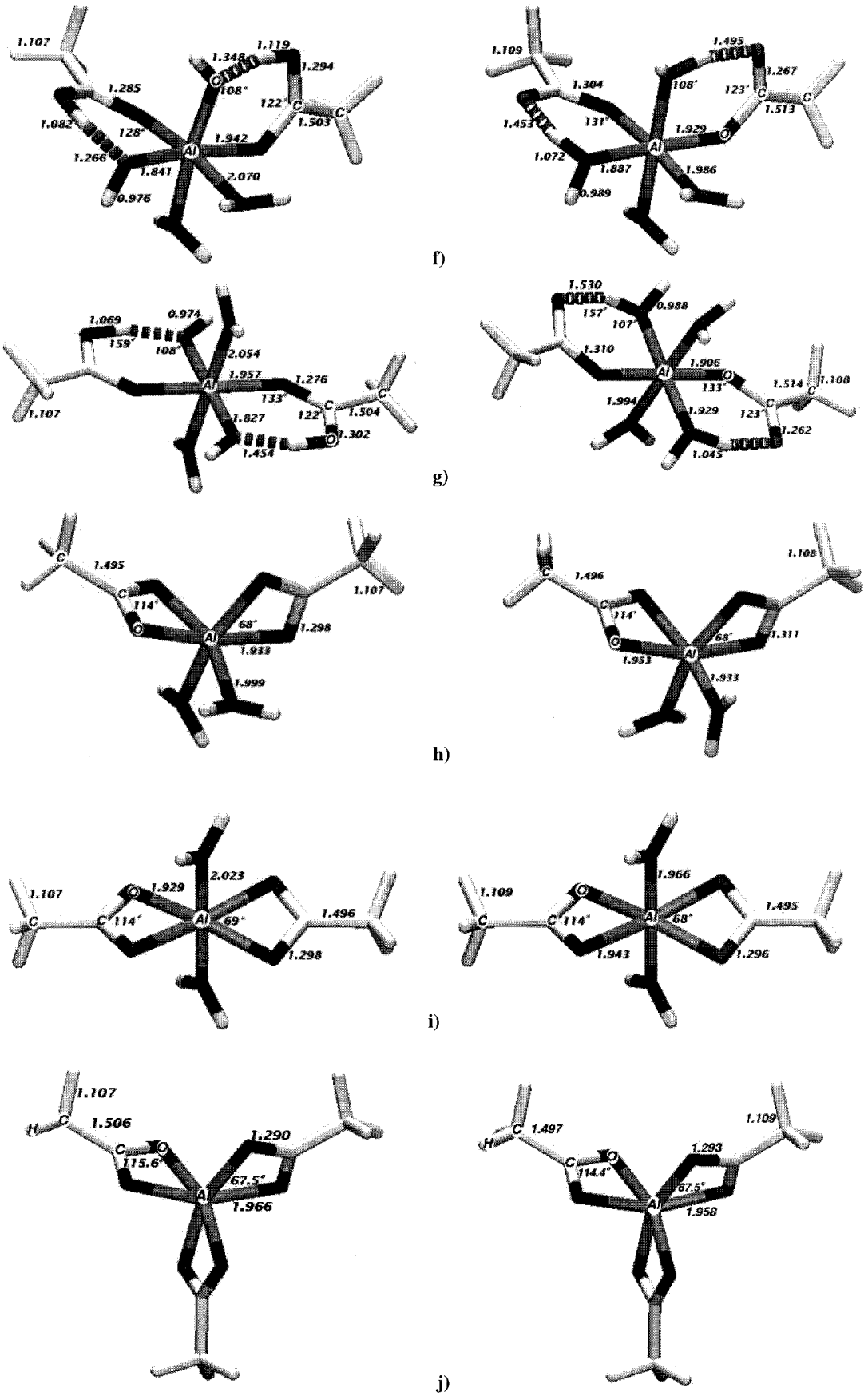


**Figure 1.** Optimized structures at the BLYP/SVP+sp level for all studied complexes in gas phase (left side) and in liquid phase (right side). Bond distances are in Å and angles are in degrees. (a) $[Al(H_2O)_6]^{3+}$, (b) $[Al(H_2O)_5OH]^{2+}$, (c) monodentate $[Al(H_2O)_5Ac]^{2+}$ and $[Al(H_2O)_4OHHAc]^{2+}$, (d) bidentate $[Al(H_2O)_4Ac]^{2+}$, (e) monodentate *cis*-$[Al(H_2O)_4AcOH]^{+}$ and *cis*-$[Al(H_2O)_3(OH)_2HAc]^{+}$, (f) monodentate *cis*-$[Al(H_2O)_4Ac_2]^{+}$ and *cis*-$[Al(H_2O)_2(OH)_2(HAc)_2]^{+}$, (g) monodentate *trans*-$[Al(H_2O)_4Ac_2]^{+}$ and *trans*-$[Al(H_2O)_2(OH)_2(HAc)_2]^{+}$, (h) bidentate *cis*-$[Al(H_2O)_2Ac_2]^{+}$, (i) *trans*-bidentate $[Al(H_2O)_2Ac_2]^{+}$, (j) $AlAc_3$.

$$\epsilon_0 = 87.740 - 0.40008t + 9.398 \times 10^{-4}t^2 - 1.410 \times 10^{-6}t^3 \quad (2)$$

where $t$ is the temperature in °C.

### III. Results and Discussion

**A. Hydration Enthalpy of $Al^{3+}$: Test of Computational Methodology.** The first part our work was focused on the selection of an appropriate DFT functional and an efficient basis set. These calculations were performed on the $[Al(H_2O)_6]^{3+}$ complex. These test calculations were carried out for the isolated complex (gas phase). Structures and formation energies $\Delta E_f(g)$ were determined according to the following reaction scheme

$$Al^{3+}(g) + 6H_2O(g) \rightarrow [Al(H_2O)_6]^{3+}(g) \quad (3)$$

Calculated structures and $\Delta E_f(g)$ values obtained with various functionals are displayed in Table 2. MP2 results are given for comparison and used as reference data for the selection of an appropriate DFT functional. One finds a slight overestimation of bond distances (except for the SVWN functional) by DFT in relation to MP2. A comparison of formation energies given in Table 2 shows that the BVWN and SVWN results deviate strongly from MP2 and that BVWNP and BLYP are closest. Hence, the following calculations were carried out with the BVWNP and/or BLYP functionals, respectively.

The results of our basis set investigations are collected in Table 3 for geometries and in Table 4 for formation energies. Table 3 shows that the geometries are relatively insensitive with respect to the basis set. The use of the augmented basis sets SVP+sp and SVP+spd causes only a very slight elongation of the Al−O distance and has negligible effect on the O−H distance and the H−O−H angle in the water molecules. On the other hand, the formation energies show a nonnegligible dependence on basis sets and clearly document the need for a systematic investigation.

One can see that the smaller SVP and DZP basis sets greatly overestimate the interaction energy by ≈50 kcal/mol as compared to the TZP and larger basis sets. The values around −700 kcal/mol obtained with the larger basis sets are also very close to the MP2/TZP energy of −705.3 kcal/mol shown in Table 2. After the addition of one diffuse set of s and p functions to the SVP basis of oxygen (SVP+sp), a drastic shift of the formation energy is observed. Also the BSSE decreases considerably (−6.8 kcal/mol) in comparison with the standard SVP basis set (−18.6 kcal/mol). The addition of one diffuse d set (SVP+spd) on oxygen atom does not significantly affect the interaction energy but decreases the $\Delta E_{BSSE}$ value further to about −3.4 kcal/mol. The $\Delta E_{BSSE}$ values for SVP+sp and SVP+spd are even smaller than for the TZP basis.

In Table 5, results from calculations in the literature are compared with our data. The most extended previous MP2 calculations by Wasserman et al.[15] give an interaction energy of −710.6 kcal/mol which is in good agreement with our MP2/TZP value of −705.3 kcal/mol. One can also see from Table 5 that the BLYP/SVP+sp and BVWNP/SVP+sp results are very similar. Because of the slightly closer value of the formation energy to MP2/TZP result, we decided to use in all following calculations the BLYP/SVP+sp combination.

The hydration enthalpy $\Delta H_{gas}$ is calculated by standard procedures within the rigid rotor/harmonic oscillator/ideal gas approximation as

$$\Delta H_{gas} = \Delta E_f + \Delta E_{ZPE} + \Delta c_v T + \Delta(RT) \quad (4)$$

**TABLE 2: Optimized Geometries and Formation Energies $\Delta E_f$ of the $[Al(H_2O)_6]^{3+}$ Cation in $T_h$ Symmetry Using Various DFT Methods and the MP2 Approach Together with the TZP Basis Set**

| method | $R$(Al−O) (Å) | $R$(O−H) (Å) | $\phi$(H−O−H) (deg) | $-\Delta E_f$ (kcal/mol) |
|---|---|---|---|---|
| BVWN | 1.980 | 0.980 | 107.0 | 672.7 |
| SVWN | 1.908 | 0.987 | 107.7 | 768.7 |
| BVWNP | 1.951 | 0.983 | 107.2 | 701.5 |
| BLYP | 1.963 | 0.985 | 107.1 | 704.6 |
| B3LYP | 1.942 | 0.977 | 107.1 | 712.7 |
| MP2 | 1.930 | 0.975 | 106.5 | 705.3 |

**TABLE 3: Optimized Geometries of the $[Al(H_2O)_6]^{3+}$ Complex in $T_h$ Symmetry Using the BVWNP Functional Together with Selected Basis Sets**

| basis set | $R$(Al−O) (Å) | $R$(O−H) (Å) | $\phi$(H−O−H) (deg) |
|---|---|---|---|
| SVP | 1.945 | 0.988 | 106.4 |
| SVP+sp | 1.952 | 0.989 | 106.2 |
| SVP+spd | 1.950 | 0.984 | 106.9 |
| DZP | 1.943 | 0.989 | 106.1 |
| TZP | 1.951 | 0.984 | 107.1 |
| TZVP | 1.951 | 0.984 | 107.1 |
| TZVPP | 1.947 | 0.981 | 107.0 |
| QZP(O) | 1.947 | 0.981 | 107.0 |

**TABLE 4: Calculated Formation Energies $\Delta E_f$ and Basis Set Superposition Error (BSSE) and BSSE-Corrected Formation Energies $\Delta E_f^{corr}$ (in kcal/mol) of the $[Al(H_2O)_6]^{3+}$ Complex Using the BVWNP Functional and Selected Basis Sets**

| basis set | $-\Delta E_f$ | $-\Delta E_{BSSE}$ | $-\Delta E_f^{corr}$ |
|---|---|---|---|
| SVP | 747.2 | 18.6 | 728.7 |
| SVP+sp | 698.7 | 6.8 | 691.9 |
| SVP+spd | 696.2 | 3.4 | 692.8 |
| DZP | 749.9 | | |
| TZP | 701.5 | 10.7 | 690.8 |
| TZVP | 700.5 | | |
| TZVPP | 696.3 | | |
| QZP(O) | 697.3 | 3.7 | 693.6 |

**TABLE 5: Calculated Structures and Formation Energies for the $[Al(H_2O)_6]^{3+}$ Cation**

| method/basis set | $R$(Al−O) (Å) | $R$(O−H) (Å) | $\phi$(H−O−H) (deg) | $-\Delta E_f$ (kcal/mol) | ref |
|---|---|---|---|---|---|
| HF/DZP | 1.824 | 0.96 | fixed | 659.9 | 11[a] |
| | 1.827 | | | | |
| | 1.914 | | | | |
| BLYP/DNP[b] | 1.961 | 1.006 | 106.8 | 682.6 | 17 |
| HF/3-21G** | 1.912 | 0.954 | 109.0 | 666.4[c] | 18 |
| MP2/6-311+G** | 1.930 | 0.974 | 106.0 | 672.1[c] | 18 |
| MP2/cc-pVDZ[d] | 1.956 | 0.979 | 106.0 | 729.0 | 15 |
| MP2/cc-pVTZ[d] | 1.907 | 0.973 | 106.5 | 710.6 | 15 |
| BLYP/SVP+sp | 1.961 | 0.991 | 106.1 | 701.5 | this work |
| BVWNP/SVP+sp | 1.952 | 0.989 | 106.2 | 698.7 | this work |
| MP2/TZP | 1.930 | 0.975 | 106.5 | 705.3 | this work |

[a] $D_{2h}$ symmetry. [b] "Double numerical" basis set + polarization function. [c] ZPE corrected. [d] Correlation consistent basis set of double and triple-ζ quality.

where $\Delta E_{ZPE}$ is the zero-point energy correction, $\Delta c_v T$ represents the heat capacity contribution, and $\Delta(RT)$ is the work term. Unfortunately, experimental gas phase hydration enthalpies are not available. For the liquid phase, the standard hydration enthalpy $\Delta H^o_{hyd}$ has been determined using mostly calorimetric measurements.[32]

In analogy to the work of Åkesson et al.[12] we use the following Born−Haber cycle

**TABLE 6: Calculated Formation Energies, Enthalpies, and Gibbs Free Energies for the $[Al(H_2O)_6]^{3+}$ Complex at the BLYP/SVP+sp Level**

| energy (kcal/mol) | gas phase | liquid phase (method a) |
|---|---|---|
| $\Delta E_f$ | −701.5 | −1128.5 |
| $\Delta E_{BSSE}$ | −6.8 | −6.8[a] |
| $\Delta E_{f/BSSE} = \Delta E_f - \Delta E_{BSSE}$ | −694.8 | −1121.7 |
| $\Delta E_0 = \Delta E_{f/BSSE} + \Delta E_{ZPE}$ | −677.1 | −1109.2 |
| $\Delta E_{298.16} = \Delta E_0 + \Delta(c_vT)$ | −680.1 | −1112.0 |
| $\Delta H^o_f = \Delta E_{298.16} + \Delta(RT)$ | −683.7 | −1116.2 |
| $\Delta G^o_f = \Delta H^o_f - \Delta(TS^\circ)$ | −622.3 | −1054.9 |

[a] The gas phase $\Delta E_{BSSE}$ was taken also for the liquid phase.

in order to compute the hydration enthalpy as follows:

$$\begin{array}{ccc} Al^{3+}(g) + 6H_2O(g) & \xrightarrow{\Delta H_{gas}} & [Al(H_2O)_6]^{3+}(g) \\ \uparrow 6\Delta H_{vap} & & \downarrow \Delta H_{solv} \\ Al^{3+}(g) + 6H_2O(l) & \xrightarrow{\Delta H^o_{hyd}} & [Al(H_2O)_6]^{3+}(l) \end{array}$$

$$\Delta H^o_{hyd} = \Delta H_{gas} + \Delta H_{solv} - 6\Delta H_{vap} \quad (5)$$

The $\Delta H_{solv}$ term in the Born−Haber cycle was replaced by the calculated free solvation energy $\Delta E_{solv}$ of the complex as computed by the PCM model. For the heat of vaporization of water ($\Delta H_{vap}$) the calculated solvation energy of the water molecule was taken. For comparison, the experimental $\Delta H_{vap}$ value at 298.16 K is −10.5 kcal/mol, our calculated PCM BLYP/SVP+sp solvation energy of the water is −6.8 kcal/mol (see Table 8). For both cases (gas and liquid phase calculations), the thermochemical analysis was carried out at $T = 298.16$ K. Results of these calculations are presented in Table 6. The difference in the $\Delta E_f$ values between gas and liquid phase is the solvation energy $\Delta E_{solv}$. This contribution is very large and represents more than $^1/_3$ of the hydration enthalpy. The second largest contribution to the hydration enthalpy is the zero-point vibrational energy correction $\Delta E_{ZPE}$ and is about 12−17 kcal/mol for solution and gas phase, respectively. The main contribution to $\Delta E_{solv}$ comes from the $[Al(H_2O)_6]^{3+}$ cation which has the solvation energy of −467.5 kcal/mol (Table 8). This high value is of course caused by the high charge of this complex. The hydration enthalpy $\Delta H^o_{hyd}$ of the $Al^{3+}$ cation can be calculated in two ways. In method a, the calculated gas phase thermodynamic values are taken and the solvation energy is added: $\Delta H^o_{hyd} = \Delta H^o_f(g) + \Delta E_{solv} = -1110.6$ kcal/mol or, in method b the thermodynamic calculation (i.e., first of all the vibrational analysis) is performed consistently for the liquid phase also and $\Delta H^o_{hyd} = \Delta H^o_f(l) = -1116.2$ kcal/mol. Both calculated values include the correction of the basis set superposition error (we took the same $\Delta E_{BSSE}$ for gas and PCM calculations). The small difference between methods a and b comes mainly from the different zero-point vibrational energy $\Delta E_{ZPE}$ for gas and liquid phase. The advantage of method a over b is the enhanced computational efficiency of the former method. The experimental value of the hydration enthalpy of the $Al^{3+}$ cation is $-1115 \pm 2$ kcal/mol.[32] Both of our calculated standard hydration enthalpies are in excellent agreement with this experimental value. They are also in very good agreement with the value of $-1106 \pm 2$ kcal/mol obtained from the molecular dynamics simulation.[15]

We have also calculated the temperature dependence of the thermodynamic quantities. Method a was used for the evaluation of the hydration enthalpy and the Gibbs free energy. The calculation of solvation energies was performed with $\epsilon_0$ values corresponding to the specific temperatures. Results are presented in Table 7 together with themodynamic gas phase quantities. One can see that the enthalpy of formation varies very little with increasing temperature. It is caused by the very small contribution of the heat capacity and the work term (eq 4) and by the weak temperature dependence of $\Delta E_{solv}$. The free energy of formation increases significantly with increasing temperature due to the contribution of the entropy factor $T\Delta S$. These trends are at least in qualitative accordance with observed thermodynamic quantities derived from solubility measurements of gibbsite in acidic sodium chloride solution[6] ($Al(OH)_3$(cryst) + $3H^+ \rightarrow Al^{3+} + 3H_2O$) where the hydrated $Al^{3+}$ cation is formed. The measured $\Delta G$ of this dissolution changes from −10.6 kcal/mol at 25 °C to −6.9 kcal/mol at 100 °C (difference 3.7 kcal/mol). Our calculated difference of $\Delta G_f$ between 25 and 100 °C is 15.1 kcal/mol (see Table 7). However, one has to be cautious with direct comparisons since the dissolution of gibbsite may not result in pure formation of the aluminum−hexaaquo complex. This reaction can be accompanied by additional complexation reactions such as formation of some aluminum hydroxoaquo complexes.

**TABLE 7: Calculated Temperature Dependence of Thermodynamic Quantities for the Formation of the $[Al(H_2O)_6]^{3+}$ Complex (BLYP/SVP+sp Level)[a]**

| | | 298.15 K | 323.15 K | 348.15 K | 373.15 K |
|---|---|---|---|---|---|
| | $\epsilon_0$ | 78.48 | 69.91 | 62.43 | 55.72 |
| gas phase | $\Delta H_f$ (kcal/mol) | −683.7 | −683.6 | −683.5 | −683.3 |
| | $\Delta G_f$ (kcal/mol) | −622.3 | −617.2 | −612.2 | −606.9 |
| liquid phase | $\Delta H_f$ (kcal/mol) | −1110.6 | −1110.6 | −1110.7 | −1110.5 |
| | $\Delta G_f$ (kcal/mol) | −1049.2 | −1044.2 | −1041.4 | −1034.1 |

[a] $\Delta H_f$ and $\Delta G_f$ values are BSSE corrected.

**TABLE 8: Calculated Solvation Energies $E_{Solv}$ and Formation Energies, Formation Enthalpies, and Formation Gibbs Free Energies in Gas and Liquid Phase According to Eq 6 (Energies in kcal/mol)**

Gas Phase

| molecule[a] | $E_{solv}$ | $\Delta E_f$(l) | $\Delta H_f$(l) | $\Delta G_f$(l) |
|---|---|---|---|---|
| $H_2O$ | −6.8 | | | |
| $OH^-$ | −104.7 | | | |
| $[Ac]^-$ | −69.8 | | | |
| $[Al(H_2O)_6]^{3+}$ | −467.5 | −701.5 | −690.5 | −629.1 |
| $[Al(H_2O)_5OH]^{2+}$ | −210.8 | −1049.2 | −1038.6 | −980.6 |
| m-$[Al(H_2O)_4OHHAc]^{2+}$ | −198.2 | −1028.5 | −1017.6 | −958.0 |
| b-$[Al(H_2O)_4Ac]^{2+}$ | −204.1 | −1001.9 | −993.0 | −940.7 |
| *cis*-m-$[Al(H_2O)_3(OH)_2HAc]^+$ | −63.0 | −1276.3 | −1265.7 | −1205.6 |
| *cis*-m-$[Al(H_2O)_2(OH)_2(HAc)_2]^+$ | −59.7 | −1249.2 | −1239.5 | −1174.8 |
| *trans*-m-$[Al(H_2O)_2(OH)_2(HAc)_2]^+$ | −56.5 | −1254.1 | −1243.8 | −1180.9 |
| *cis*-b-$[Al(H_2O)_2(Ac)_2]^+$ | −59.9 | −1212.0 | −1203.8 | −1160.9 |
| *trans*-b-$[Al(H_2O)_2(Ac)_2]^+$ | −57.1 | −1209.5 | −1201.6 | −1159.6 |
| b-$AlAc_3$ | −4.1 | −1333.2 | −1327.5 | −1289.5 |

Liquid Phase

| molecule[a] | $\Delta E_f$(l) | $\Delta H_f$(l) | $\Delta G_f$(l) |
|---|---|---|---|
| $[Al(H_2O)_6]^{3+}$ | −1128.5 | −1117.4 | −1056.1 |
| $[Al(H_2O)_5OH]^{2+}$ | −1121.5 | −1110.9 | −1052.9 |
| m-$[Al(H_2O)_5Ac]^{2+}$ | −1123.1 | −1112.2 | −1052.6 |
| b-$[Al(H_2O)_4Ac]^{2+}$ | −1109.1 | −1100.3 | −1048.0 |
| *cis*-m-$[Al(H_2O)_4AcOH]^+$ | −1139.7 | −1129.1 | −1068.9 |
| *cis*-m-$[AlH_2O)_4(Ac)_2]^+$ | −1142.4 | −1132.7 | −1068.0 |
| *trans*-m-$[AlH_2O)_4(Ac)_2]^+$ | −1144.0 | −1133.7 | −1070.8 |
| *cis*-b-$[Al(H_2O)_2(Ac)_2]^+$ | −1118.8 | −1110.7 | −1067.8 |
| *trans*-b-$[Al(H_2O)_2(Ac)_2]^+$ | −1113.6 | −1105.7 | −1063.6 |
| b-$AlAc_3$ | −1128.0 | −1122.3 | −1084.3 |

[a] m = monodentate; b = bidentate.

**B. Formation of the Aqueous Aluminum−Acetate Complexes.** The calculations on the aluminum−hexaaquo complex

**TABLE 9: Formation Reactions of Aluminum−Acetate Complexes: Calculated Reaction Energies, Enthalpies, and Gibbs Free Energies for Gas and Liquid Phase (Energies in kcal/mol)**

| gas phase reactions[a] | $\Delta E_r$(g) | $\Delta H_r$(g) | $\Delta G_r$(g) | no. |
|---|---|---|---|---|
| $OH^- + [Al(H_2O)_6]^{3+} \rightarrow [Al(H_2O)_5OH]^{2+} + H_2O$ | −347.7 | −348.1 | −351.4 | 9 |
| $[Ac]^- + [Al(H_2O)_6]^{3+} \rightarrow$ m-$[Al(H_2O)_4OHHAc]^{2+} + H_2O$ | −326.9 | −327.1 | −328.8 | 10 |
| $[Ac]^- + [Al(H_2O)_6]^{3+} \rightarrow$ b-$[Al(H_2O)_4Ac]^{2+} + 2H_2O$ | −300.3 | 303.8 | −311.6 | 11 |
| $[Ac]^- + [Al(H_2O)_5OH]^{2+} \rightarrow$ *cis*-m-$[Al(H_2O)_3(OH)_2HAc]^+ + H_2O$ | −227.1 | −227.2 | −225.0 | 12 |
| $2[Ac]^- + [Al(H_2O)_6]^{3+} \rightarrow$ *cis*-m-$[Al(H_2O)_2(OH)_2(HAc)_2]^+ + 2H_2O$ | −547.7 | −549.1 | −545.7 | 13 |
| $2[Ac]^- + [Al(H_2O)_6]^{3+} \rightarrow$ *trans*-m-$[Al(H_2O)_2(OH)_2(HAc)_2]^+ + 2H_2O$ | −552.5 | −553.3 | −551.7 | 14 |
| $2[Ac]^- + [Al(H_2O)_6]^{3+} \rightarrow$ *cis*-b-$[Al(H_2O)_2Ac_2]^+ + 4H_2O$ | −510.4 | −513.4 | −531.8 | 15 |
| $2[Ac]^- + [Al(H_2O)_6]^{3+} \rightarrow$ *trans*-b-$[Al(H_2O)_2Ac_2]^+ + 4\ H_2O$ | −508.0 | −511.2 | −530.4 | 16 |
| $3[Ac]^- + [Al(H_2O)_6]^{3+} \rightarrow$ b-$AlAc_3 + 6H_2O$ | −631.7 | −637.1 | −660.4 | 17 |
| **liquid phase reactions[a]** | $\Delta E_r$(l) | $\Delta H_r$(l) | $\Delta G_r$(l) | no. |
| $OH^- + [Al(H_2O)_6]^{3+} \rightarrow [Al(H_2O)_5OH]^{2+} + H_2O$ | 7.0 | 6.5 | 3.2 | 9 |
| $[Ac]^- + [Al(H_2O)_6]^{3+} \rightarrow$ m-$[Al(H_2O)_5Ac]^{2+} + H_2O$ | 5.4 | 5.2 | 3.5 | 10 |
| $[Ac]^- + [Al(H_2O)_6]^{3+} \rightarrow$ b-$[Al(H_2O)_4Ac]^{2+} + 2H_2O$ | 19.4 | 15.9 | 8.1 | 11 |
| $[Ac]^- + [Al(H_2O)_5OH]^{2+} \rightarrow$ *cis*-m-$[Al(H_2O)_4AcOH]^+ + H_2O$ | −18.2 | −18.2 | −16.1 | 12 |
| $2[Ac]^- + [Al(H_2O)_6]^{3+} \rightarrow$ *cis*-m-$[Al(H_2O)_4Ac_2]^+ + 2H_2O$ | −13.9 | −15.3 | −11.9 | 13 |
| $2[Ac]^- + [Al(H_2O)_6]^{3+} \rightarrow$ *trans*-m-$[Al(H_2O)_4Ac_2]^+ + 2H_2O$ | −15.5 | −16.3 | −14.7 | 14 |
| $2[Ac]^- + [Al(H_2O)_6]^{3+} \rightarrow$ *cis*-b-$[Al(H_2O)_2Ac_2]^+ + 4H_2O$ | 9.7 | 6.8 | −11.7 | 15 |
| $2[Ac]^- + [Al(H_2O)_6]^{3+} \rightarrow$ *trans*-b-$[Al(H_2O)_2Ac_2]^+ + 4H_2O$ | 14.9 | 11.8 | −7.5 | 16 |
| $3[Ac]^- + [Al(H_2O)_6]^{3+} \rightarrow$ b-$AlAc_3 + 6H_2O$ | 0.5 | −4.9 | −28.2 | 17 |

[a] m = monodentate; b = bidentate.

demonstrated the importance of the solvation energies. Other contributions were much smaller and played a minor role. The difference between $\Delta E_f$(l) and $\Delta H^o_f$(l) is about 12 kcal/mol as compared to the 427 kcal/mol of the solvation energy (see Table 6). Moreover, the difference in the calculated hydration enthalpy of the $Al^{3+}$ cation by the methods a and b is only 6 kcal/mol. These relations are certainly also valid for the aqueous aluminum−acetate complexes. Hence, in the calculations on these complexes we followed method a and performed the thermochemical calculations for efficiency reasons on the gas phase complexes and added to them the solvation energies of these complexes. All calculated values are computed for 298.15 K. Also, the analysis of the basis set superposition error was not performed anymore. We expect here similar BSSE values as for the aluminum−hexaaquo complex. Moreover, having a 6-fold coordinated aluminum cation on both sides of the complexation reactions (Table 9), this error will be mostly canceled.

All studied aqueous aluminum complexes are displayed in Figure 1. Important structural parameters are given also in the figure. The formation energies $\Delta E_f$ for these complexes in both phases and the solvation energies, $E_{solv}$, are collected in Table 8. The formation energies $\Delta E_f$ of these complexes were calculated in analogy to eq 3 according to the following reactions schemes:

gas phase

$$Al^{3+}(g) + pH_2O(g) + qAc^-(g) + rOH^-(g) \rightarrow [Al(H_2O)_pAc_qOH_r]^{(3-q-r)+}(g) \quad (6)$$

liquid phase

$$Al^{3+}(g) + pH_2O(l) + qAc^-(l) + rOH^-(l) \rightarrow [Al(H_2O)_pAc_qOH_r]^{(3-q-r)+}(l) \quad (7)$$

The first observation we want to make is that an intramolecular proton transfer occurred in all monodentate structures in the gas phase. The proton belonging to a water molecule adjacent to the free oxygen atom of the acetate carboxyl group moved to this oxygen atom, leading to two new ligands (acetic acid and hydroxyl anion) instead of the two original ones (water molecule and acetate anion). Hence, we have obtained three new complexes in the gas phase: $[Al(H_2O)_4OHHAc]^{2+}$, *cis*-$[Al(H_2O)_2(OH)_2(HAc)_2]^{2+}$, and *trans*-$[Al(H_2O)_2(OH)_2(HAc)_2]^{2+}$. The optimization procedure was started from the acetate structure and resulted directly in the proton transfer. A local minimum for the original structure without proton transfer could not be found. In contrast to these gas phase results, we found in the PCM calculations a stationary point for the original monodentate structure. However, another stationary point could be located for the structure $[Al(H_2O)_4OHHAc]^{2+}$ where proton transfer had occurred. It was 4 kcal/mol higher than the original $[Al(H_2O)_5Ac]^{2+}$ complex. These intramolecular proton transfer structures were not observed in the gas phase calculations by Kubicki et al.[18] who had used a smaller basis set and the SCF method for the geometry optimizations. We reduced the basis set also to SV quality. When the DFT method was used, the same proton transfer was observed as before. With the SCF method, no proton transfer was observed. Since the functionals used here were carefully selected in comparison with MP2 calculations for the aluminum−hexaaquo complex, we think that the DFT calculations give the correct results. However, it would be interesting to perform MP2 calculations on the acetate complexes also. Unfortunately, such calculations were too demanding and not possible with our available computer resources. A final decision about the feasibility of the proton transfer would also require the determination of the barrier height between the two structures.

The result of the proton transfer is a shortening of the Al−OH bond by approximately 0.1−0.2 Å in comparison with Al−$OH_2$ bond lengths. This is in agreement with our results obtained for the aqueous monohydroxoaluminum complex where a value of 1.713 Å for the Al−OH bond length was obtained which is shorter than the average value of 2.007 Å for Al−$OH_2$ bond length in this complex. This is also in agreement with the calculations of Kubicki et al.[18] where a value 1.76 Å for the Al−O bond length in the $[Al(OH)_4]^-$ complex and the value of 1.91 Å in the $[Al(H_2O)_6]^{3+}$ complex were obtained at the HF/3-21G** level.

The Al−O bond lengths with the O atom from carboxyl groups are shorter than Al−O bond lengths with O atom from water molecules in all aluminum−acetate complexes for gas

phase and in solution. The Al−O bond length is also shorter in the monodentate structure as compared to the bidentate one. This shortening is less pronounced in complexes with two $Ac^-$ ligands as compared to complexes with one $Ac^-$ anion. The $Al-OH_2$ bond lengths in aluminum−acetate complexes are on the average longer than those in the $[Al(H_2O)_6]^{3+}$ complex. The formation of Al−O−C linkages lengthens the C−O bonds and shortens the C−C bonds in all studied cases in comparison with the free $Ac^-$ anion (both gas and liquid phase). The average C−O distance is 1.270 Å and the average C−C distance is 1.581 Å for the gas phase, and 1.274 and 1.543 Å for liquid phase. The C−O bonds in the Al−O−C linkage in the monodentate species are longer than the other C−O bonds in cases when no proton transfer was observed. On the other hand, when the intramolecular proton transfer occurred and an acetic acid ligand was formed, both C−O bond lengths in this ligand became similar. The O−C−O angles in $Ac^-$ ligands (about 122° for monodentate and 114° for bidentate complexes) are smaller than in the free $Ac^-$ anion (128.7° for the gas and 125.4° for the liquid phase). These values are relatively constant in all investigated structures and phases. All observed structural changes in aluminum acetate complexes are in the accordance with observations by Kubicki et al.[18] except the aforementioned intramolecular proton transfer.

Similar effects as described above were observed also for mixed hydroxoacetate complex $[Al(H_2O)_4AcOH]^+$. The intramolecular proton transfer occurred in the gas phase and hence, the new complex $[Al(H_2O)_3(OH)_2HAc]^+$ with $2OH^-$ ligands and one acetic acid ligand was formed. Again, this proton transfer was not observed in the liquid phase. The structural changes are very similar to those in other monodentate species (see Figure 1).

The solvent effect is reflected in the following structural changes: (i) the Al−O bonds (both with acetate anion and water) are shortened; (ii) the C−O bonds in Al−O−C linkages are also shortened (except the cases, where intramolecular proton transfer occurred); and (iii) the C−C bond length is slightly stretched. An opposite solvent effect on the Al−O bond has been reported by Marcos et al.[10] for the aluminum−hexaaquo complex. We suspect that this discrepancy comes from the fact that in their work the cavity volume was kept constant during geometry optimization. The Al−O bond distance of 1.92 Å (see Figure 1) is in good agreement with the experimental one of 1.89 Å[33] derived from X-ray diffraction studies of solutions. Generally, structural changes due to the solvent effect decrease with decreasing charge of the complexes (compare the value of 1.966 Å for the Al−O bond in the gas and 1.958 Å in the liquid phase for the $AlAc_3$ complex and with those of 1.961 and 1.920 Å for the aluminum−hexaaquo complex in the gas phase and in solution, respectively).

Now we want to discuss the energetical aspects of the studied complexes and their respective reactions. The solvation energy $E_{solv}$ given in Table 8 is defined as the difference of the energies of the optimized structures with and without the PCM model. The solvation energy correlates with the charge of the chemical species and decreases in absolute value with decreasing charge. The $\Delta E_f$ values for the reaction schemes (6) and (7) shown in Table 8 are used to evaluate the stability of the aluminum−acetate complexes. These values are strongly affected by solvation energies. In the gas phase the stability of the complexes is quite clear: $Ac_3 > Ac_2 > Ac_1 > [Al(H_2O)_6]^{3+}$. When the monodentate and bidentate species are compared, the first ones are more stable than the second ones by about 26 kcal/mol in the case of one $Ac^-$ ligand and about 40 kcal/mol in the case of two $Ac^-$ ligands. This stronger stabilization of the monodentate species can be assigned to the stronger Al−O−H bond which has formed because of the aforementioned proton transfer and the formation of an intramolecular hydrogen bond. One can also see from Table 8 that the hydroxoaluminum complex $[Al(H_2O)_5OH]^{2+}$ is more stable in the gas phase than the monodentate aluminum−acetate complex $[Al(H_2O)_4OHHAc]^{2+}$ by about 21 kcal/mol. The intramolecular hydrogen bond and a strong Al−O−H bond cause the mixed hydroxoacetate complex $[Al(H_2O)_3(OH)_2HAc]^+$ to be the second most stable complex in the gas phase. The same order of stability in the gas phase is also found for the $\Delta H_f$ and $\Delta G_f$ values presented in Table 8.

In the liquid phase the differences in $\Delta E_f$ are not so pronounced and a simple ordering of the stability of the acetate complexes as for the gas phase cannot be given. All formation energies fall into an interval of about 35 kcal/mol. As in the gas phase, the monodentate species are more stable than the bidentate ones, although the differences are not so large. According to formation energies $\Delta E_f$, the monodentate complexes with two ligands ($[Al(H_2O)_4AcOH]^+$ and $[Al(H_2O)_4Ac_2]^+$) are the most stable ones in the liquid phase. The differences between cis and trans isomers are small (up to 5 kcal/mol) both for mono- and bidentate species. While the cis isomer of the monodentate Al−diacetate complex is more stable in the gas phase than the trans isomer, the reverse is true in the liquid phase. However, the difference is only 1.6 kcal/mol. The situation is different for bidentate species. The cis isomer is more stable than the trans isomer in both cases (gas and liquid). Comparing gas and liquid phase formation energies, one can see that $[Al(H_2O)_6]^{3+}$, $[Al(H_2O)_5Ac]^{2+}$, and $[Al(H_2O)_5OH]^{2+}$ are more stable in the liquid phase while the remaining complexes are more stable in the gas phase. This situation can be explained according to eq 7 by the relative magnitudes of the solvation energies of water and acetate on the one side and of the acetate complex on the other side.

The Al−acetate complexes have been studied experimentally by means of solubility and potentiometric measurements.[5−9] $\Delta G$ and $\Delta H$ values for the reactions

$$Al^{3+} + nAc^- \rightarrow Al(Ac)_n^{3-n} \; (n = 1, 2) \qquad (8)$$

in aqueous solutions have been determined. Since under certain experimental conditions the hydrolysis of the $Al^{3+}$ cation becomes important and hydroxo complexes are formed in the solution, also mixed hydroxoacetate complexes[9] have been considered. The occurrence of the triacetate complex is also reported even though quantitative data could not be given in this case.[8,9] From these experiments there is no information available whether these complexes occur as monodentate or bidentate structures. We identify the global reaction scheme (8) given in the experimental work with the specific substitution of water molecules in the aluminum−hexaaquo complex by $n$ acetate anions. The various possibilities, which were finally selected, are listed in Table 9 together with respective reaction energy values $\Delta E_r$. One can see from that table that these reactions have very high negative reaction energies in the gas phase and that solvent effects play a crucial role again.

Comparing $\Delta E_r$ or $\Delta H_r$ values for the liquid phase, one can see that the formation of monodentate complexes is more favorable than that of bidentate complexes. This is consistent with conclusions from calculations by Kubicki at al.[18] and with the observation of Yang at al.[34] that a large strain energy is connected with the formation of the four-membered ring in bidentate acetate complexes with small metal cations. The situation changes when $\Delta G$ values are compared. Large differ-

ences between $\Delta H$ and $\Delta G$ are observed for the formation of bidentate species whereas much smaller differences occur in the case of the monodentate structures. This lowering of $\Delta G$ is caused by the large positive reactions entropies when bidentate complexes are formed. It is found for all mono-, di-, and triacetate bidentate complexes. The change of entropy is connected with the replacement of two water molecules per acetate during the formation of bidentate species as opposed to monodentate species where only one water molecule per acetate anion is released. According to $\Delta G$ values, the formation of bidentate complexes becomes favorable. In fact, the most stable one is the bidentate triacetate complex. With increasing temperature the entropy factor will become even more dominant. Experimentally, the triacetate complex is observed only at temperatures above 100° C.[9] We suppose that the formation of the bidentate triacetate complex is inhibited by a relatively high energy barrier which is only overcome at higher temperatures. Our calculations also demonstrate the significance of the mixed hydroxo-acetate complex. This is in good agreement with the work of Benezeth at al.[9] where the occurrence of this complex was reported.

For the formation of the monoacetate complex ($AlAc^{2+}$), Palmer and Bell[8] obtain an experimental $\Delta H$ value of $+4 \pm 1.4$ kcal/mol and a $\Delta G$ value of $-3.8 \pm 0.2$ kcal/mol at 25 °C. The calculated $\Delta H$ value for the monodentate structure (see reaction 10 in Table 9) of 5.2 kcal/mol is in good agreement with the experimental one. For comparison, in the work by Kubicki et al.[20] a value of $-40.2$ kcal/mol was obtained for the reaction energy using explicitly solvated $Ac^-$ and $H_2O$ molecules in conjunction with the SCIPCM[35] solvation model. This value represented a big improvement with respect to the original results disregarding solvation effects, but is still significantly off from the experimental value.

The calculated $\Delta G$ value of 3.5 kcal/mol for the monodentate structure does not agree so well with the experimental result. However, if we look at the difference between the measured $\Delta G$ and $\Delta H$ values instead on the absolute value of $\Delta G$ we observe that this difference of $-7.8$ kcal/mol is rather large (in absolute value) and more typical for bidentate structures (see the above discussion on entropy effects and the value of $-7.8$ kcal/mol for reaction 11 in Table 9). For the diacetate complex ($AlAc_2^+$), Palmer and Bell[8] obtain a $\Delta H$ value of $+7.2 \pm 7.2$ kcal/mol and a $\Delta G$ value of $-6.2 \pm 0.7$ kcal/mol. These values and the difference of $-13.4$ kcal/mol between them are in better agreement with our calculated values for the bidentate diacetate complexes (reactions 15 and 16) than for monodentate ones (reactions 13 and 14).

Our calculated $\Delta G$ values show that monodentate complexes are only little preferred over bidentate ones. Thus, also bidentate species should be considered as significant in solution. Overall, the agreement between the experimental and our theoretical data is good but not entirely consistent. The reasons for this are, on the one hand, errors still existing in the computational procedures. But, on the other hand, we also suspect that the thermodynamical models used for the evaluation of the thermodynamic data are not flexible enough. On the basis of our results we would like to suggest a differentiation between mono- and bidentate structures in these models.

## IV. Conclusions

In our methodological study of the formation energy of the $[Al(H_2O)_6]^{3+}$ complex, several density functionals have been compared with MP2 calculations and extensive basis set investigations have been carried out. This has led to a significant elimination of systematic errors and to an efficient computational procedure, which could be applied to complexes containing acetate anions. A similar accuracy as for $[Al(H_2O)_6]^{3+}$ can be expected for the latter cases too. Even larger complexes including larger organic acids like oxalic acid and citric acid can be studied in this way.[36] In the case of the $[Al(H_2O)_6]^{3+}$ complex the solvation energy represents more than $^1/_3$ of the total hydration enthalpy. The other energetic corrections to the formation energy of the $[Al(H_2O)_6]^{3+}$ complex (zero-point vibrational energy, thermal corrections) are not so large as the solvation energy but are also required for high-accuracy results. Our calculated standard hydration enthalpy of $-1116.2$ kcal/mol at 289.16 K is in very good agreement with the experimental value of $-1115.0 \pm 2$ kcal/mol.[32] The trend of the calculated temperature dependence of the thermodynamic quantities agrees with measured enthalpies and Gibbs free energies of the dissolution of gibbsite.[6]

Molecular orbital calculations of hydrated aluminum−acetate complexes provide good insight into structures and structural changes due to solvation effects. The Al−O bond is stretched, the C−O bonds are shortened in the Al−O−C linkages (except the cases where intramolecular proton transfer occurred), and the C−C bond is slightly lengthened under solvation effects. The size of the structural changes decreases with decreasing charge of the complex. An intramolecular proton transfer was observed in all monodentate structures in the gas phase but not in the liquid phase. In general, the monodentate structures are energetically more stable than the bidentate ones. The enhanced stability of the former structures is supported by intramolecular hydrogen bonds and certainly also by unfavorable sterical factors and strain in the bidentate Al−carboxyl ring.

The formation energies and the reaction energies defined in eqs 7 and 8 depend strongly on solvation effects. Only inclusion of solvation effects into the theoretical model brings the calculated reaction energies into realistic agreement with the experimental data for solution. While in the gas phase the order of stability of the aluminum−acetate complexes is well established ($Ac_3 > Ac_2 > Ac$), this ordering is not so pronounced in the liquid phase. Calculations on the mixed hydroxoacetate complex confirmed the conclusions of Benezeth at al.[9] about the significance of this complex in solution. Comparison of calculated $\Delta H$ and $\Delta G$ values for the reactions defined by the general eq 8 and by their specific realizations given in Table 9 shows significant influence of $\Delta S$ in the case of bidentate complexes. This fact can be explained that in this case two water molecules of the aluminum−hexaaquo complex are substituted by one acetate as opposed to the monodentate case where only one water molecule is released. Thus, $\Delta H/\Delta G$ differences can be taken as an indicator for bidentate structures. From a comparison of experimental and calculated values we conclude that monodentate structures are only little preferred over bidentate ones and that we expect a relatively complicated system of chemical equilibria without any dominant complex. Unfortunately, it is not possible to investigate experimentally each reaction individually. Measurements are performed on a mixture of different reactions, and results are interpreted on the basis of certain thermodynamic models. We suggest that in these models one should not only distinguish between mono-, bi-, and triacetate complexes and/or mixed hydroxoacetate complexes but also between mono- and bidentate species.

**Acknowledgment.** This work was supported by the Austrian Science Fund, project no. P12969-CHE. We are grateful for

technical support and computer time at the DEC Alpha server of the computer center of the University of Vienna.

## References and Notes

(1) Kinraide, T. B.; Parker, D. R. *Phys. Plant* **1990**, *79*, 283.
(2) Parker, D. R.; Bretsch, P. M. *Environ. Sci. Technol.* **1992**, *26*, 908.
(3) Bollard, E. G. Involvement of unusual elements in plant groth and nutrition. In *Inorganic plant nutrition*; Läuchli, A., Bielski, R. L., Eds.; Springer-Verlag: Berlin, 1983; pp 659−744.
(4) Kharaka, Y. K.; Lawm, L. M.; Carothers, W. W.; Goerlitz, D. F. *Soc. Econ. Paleontol. Mineral. Spec. Publ.* **1986**, *38*, 111.
(5) Fein, J. B. *Geochim. Cosmochim. Acta* **1991**, *55*, 955.
(6) Palmer, D. A.; Wesolowski, D. J. *Geochim. Cosmochim. Acta* **1992**, *56*, 1093.
(7) Schock, E. L.; Koretsky, C. M. *Geochim. Cosmochim. Acta* **1993**, *57*, 4899.
(8) Palmer, D. A.; Bell, J. L. *Geochim. Cosmochim. Acta* **1994**, *58*, 651.
(9) Benezeth, P.; Castet, S.; Dandurand, J.-L.; Gout, R.; Schott, J. *Geochim. Cosmochim. Acta* **1994**, *58*, 4561.
(10) Marcos, E. S.; Pappalardo, R. R.; Rinaldi, D. *J. Phys. Chem.* **1991**, *95*, 8928.
(11) Probst, M. M.; Hermansson, K. *J. Chem. Phys.* **1992**, *96*, 8995.
(12) Åkesson, R.; Pettersson, L. M. G.; Sandström, M.; Siegbahn, P. E. M.; Wahlgren, U. J. *Phys. Chem.* **1992**, *96*, 10773.
(13) Åkesson, R.; Pettersson, L. M. G.; Sandström, M.; Wahlgren, U. J. *J. Am. Chem. Soc.* **1994**, *116*, 8691.
(14) Åkesson, R.; Pettersson, L. M. G.; Sandström, M.; Wahlgren, U. J. *J. Am. Chem.* Soc. **1994**, *116*, 8705.
(15) Wasserman, E.; Rustad, J. R.; Xantheas, S. S. *J. Chem. Phys.* **1997**, *106*, 9769.
(16) Chang, Ch. M.; Wang, M. K. *J. Mol. Struct. (THEOCHEM)* **1997**, *417*, 237.
(17) Chang, Ch. M.; Wang, M. K. *J. Mol. Struct. (THEOCHEM)* **1998**, *434*, 163.
(18) Kubicki, J. D.; Blake, G. A.; Apitz, S. E. *Geochim. Cosmochim. Acta* **1996**, *60*, 4897.
(19) Kubicki, J. D.; Blake, G. A.; Apitz, S. E. *Geochim. Cosmochim. Acta* **1997**, *61*, 1031.
(20) Kubicki, J. D.; Sykes, D.; Apitz, S. E. *J. Phys. Chem. A* **1999**, *103*, 903.
(21) Miertus, S.; Scrocco, E.; Tomasi, *J. Chem. Phys.* **1981**, *55*, 117.
(22) Miertus, S.; Tomasi, J. *Chem. Phys.* **1982**, *65*, 239.
(23) Cossi, M.; Barone, V.; Cammi, R.; Tomasi, J. *Chem. Phys. Lett.* **1996**, *255*, 327.
(24) Ahlrichs, R.; Bär, M.; Häser, M.; Horn, H.; Kölmel, C. *Chem. Phys. Lett.* **1989**, *162*, 165.
(25) Arnim, M. v.; Ahlrichs, R. *J. Comput. Chem.* **1998**, *19*, 1746.
(26) *Gaussian 98*, Revision A.7; Frisch, M. J.; Trucks, G. W.; Schlegel, H. B.; Scuseria, G. E.; Robb, M. A.; Cheeseman, J. R.; Zakrzewski, V. G.; Montgomery, J. A., Jr.; Stratmann, R. E.; Burant, J. C.; Dapprich, S.; Millam, V.; Daniels, A. D.; Kudin, K. N.; Strain, M. C.; Farkas, O.; Tomasi, J.; Barone, V.; Cossi, M.; Cammi, R.; Mennucci, C.; Pomelli, C.; Adamo, S.; Clifford, J.; Ochterski, G. A.; Petersson, P. Y.; Ayala, B.; Cui, Q.; Morokuma, K.; Malick, D. K.; Rabuck, A. D.; Raghavachari, K.; Foresman, J. B.; Cioslowski, J.; Ortiz, J. V.; Stefanov, B. B.; Liu, G.; Liashenko, A.; Piskorz, P.; Komaromi, I.; Gomperts, R.; Martin, R. L.; Fox, D. J.; Keith, T.; Al-Laham, M. A.; Peng, C. Y.; Nanayakkara, A.; Gonzalez, C.; Challacombe, M.; Gill, P. M. W.; Johnson, B.; Chen, W.; Wong, M. W.; Andres, J. L.; Gonzalez, C.; Head-Gordon, M.; Replogle, E. S.; Pople, J. A. Gaussian, Inc.: Pittsburgh, PA, 1998.
(27) Jensen, F. *Introduction to Computational Chemistry*; John Wiley: New York, 1999; pp 177−193.
(28) Schäfer, A.; Horn, H.; Ahlrichs, R. *J. Chem. Phys.* **1992**, *97*, 2571.
(29) Schäfer, A.; Huber, Ch.; Ahlrichs, R. *J. Chem. Phys.* **1994**, *100*, 5829.
(30) Boys, S. F.; Bernardi, F. *Mol. Phys.* **1970**, *19*, 553.
(31) Malmberg, C. G.; Maryott, A. A. *J. Res. Natl. Bur. Stand.* **1956**, *60*, 609.
(32) Smith, D. W. *J. Chem. Educ.* **1977**, *54*, 540.
(33) Marcus, Y. *Chem. Rev.* **1988**, *88*, 1475.
(34) Yang, M. M.; Crerar, D. A.; Irish, D. E. *Geochim. Cosmochim. Acta* **1989**, *53*, 319.
(35) Foresman, J. B.; Keith, T. A.; Wiberg, K. B.; Snoonian, J.; Frisch, M. J. *J. Phys. Chem.* **1996**, *100*, 16098.
(36) Aquino, A.; Tunega, D.; Haberhauer, G.; Gerzabek, M.; Lischka, H. *Phys. Chem. Chem. Phys*., in press.